

Surface hydroxyl groups of synthetic α -FeOOH in promoting \bullet OH generation from aqueous ozone: Property and activity relationship

Tao Zhang^a, Chunjuan Li^a, Jun Ma^{a,*}, Hai Tian^a, Zhimin Qiang^b

^a School of Municipal and Environmental Engineering, Harbin Institute of Technology, Harbin 150090, China

^b Research Center for Eco-Environmental Sciences, Chinese Academy of Sciences, Beijing 100085, China

Received 24 December 2006; received in revised form 1 January 2008; accepted 15 January 2008

Available online 20 January 2008

Abstract

This work investigated the relationship between the property of the surface hydroxyl groups of hydroxylated synthetic α -FeOOH and their catalytic activity in promoting hydroxyl radical (\bullet OH) generation from aqueous ozone. Nitrobenzene was used as an ozone-resistant probe to quantify \bullet OH generation. ATR-FTIR analysis reveals that sulfate and phosphate suppressed the catalytic activity of α -FeOOH through substituting its surface hydroxyl groups, which implies that the catalyst surface hydroxyl groups were active sites for promoting \bullet OH generation. Compared with other synthetic oxo-hydroxides such as β -FeOOH, γ -FeOOH and γ -AlOOH, α -FeOOH achieved a highest R_c value (i.e., 1.11×10^{-7} , molar concentration ratio of \bullet OH to O_3) in catalytic ozonation. No correlation could be established between the surface hydroxyl density and the \bullet OH-promoting activity of the oxo-hydroxides. In contrast, their catalytic activity was found to be reversely related to the IR stretching frequencies of surface hydroxyl groups. The results indicate that not all surface hydroxyl groups of the oxo-hydroxides possessed the same high catalytic activity, but the weak surface MeO–H bonds were favorable sites for promoting \bullet OH generation from aqueous ozone. The surface hydroxyl–ozone interaction was thus proposed for the catalyzed \bullet OH generation, which can explain why neutral surface hydroxyl species of α -FeOOH was more active than protonated or deprotonated species.

© 2008 Elsevier B.V. All rights reserved.

Keywords: Synthetic α -FeOOH; ATR-FTIR; Oxo-hydroxide; Surface hydroxyl group; Hydroxyl radical generation; Catalytic ozonation

1. Introduction

Ozone is commonly used for oxidation of organic pollutants in water treatment. It reacts fast with organic pollutants containing amino groups, activated aromatic systems, or double bonds [1,2]. However, with respect to recalcitrant organic pollutants in water, ozonation alone is not effective. Ozone-based advanced oxidation processes (AOPs) have thus been developed, including O_3/H_2O_2 , O_3/UV , and $O_3/UV/H_2O_2$, to improve the oxidation of refractory pollutants in water. More recently, catalytic ozonation with metal oxides has emerged as an alternative technique to enhance organic decomposition without extra addition of chemicals and energy into water.

Catalytic ozonation with metal oxides can proceed through two pathways: (a) enhancing \bullet OH generation from aqueous ozone [3–5] and (b) forming surface complexes between the

carboxylic groups of the pollutants and the surface metal sites of the catalyst, which renders the coordinated pollutants more reactive towards molecular ozone [6–8]. Most previous researches on catalytic ozonation have focused on the removal of low molecular-weight carboxylic compounds at low pH values. However, little effort has been made to elucidate the role of surface hydroxyl groups of the catalyst in promoting \bullet OH generation during catalytic ozonation.

When introduced into water, metal oxides tend to strongly adsorb H_2O molecules. The adsorbed H_2O dissociates into OH^- and H^+ , forming surface hydroxyl groups with the surface metal and oxygen sites, respectively [9]. Water molecules are also attached to the surface hydroxyl groups through hydrogen-bond in the outer-sphere in several layers [10]. Thus, the chemisorbed hydroxyl groups dominate the properties of the oxide/water interface and interact with O_3 and organic molecules in the catalytic ozonation. When the surface metal cations are in stable valences (e.g., Fe^{3+} and Al^{3+}) and they cannot form surface complexes with organic pollutants, the surface hydroxyl groups may play an important role in the catalytic ozonation.

* Corresponding author. Tel.: +86 451 86282292; fax: +86 451 82368074.

E-mail address: majun@hit.edu.cn (J. Ma).

Former researches have reported that goethite (α -FeOOH) could enhance ozone decomposition to generate \bullet OH in water and its surface hydroxyl groups (both charged and uncharged) were hypothesized to be active sites [5,11]. However, this hypothesis has never been substantiated by experimental data. Moreover, the relationship between the property of the surface hydroxyl groups and their activity in promoting \bullet OH generation is still largely unknown. This study was aimed to elucidate the role of the surface hydroxyl groups of metal oxides in catalyzing organic decomposition. Nitrobenzene (NB) was selected as an ozone-resistant probe ($k_{O_3, NB} = 0.09 \text{ M}^{-1} \text{ s}^{-1}$ in water [12]). Since NB is hardly adsorbed on the hydroxylated surfaces of metal oxides, it is suitable to probe the generation of \bullet OH from aqueous ozone during catalytic ozonation.

2. Experimental

2.1. Catalysts

The α -FeOOH was synthesized following Kandori et al. [13], and the β -FeOOH and γ -FeOOH were synthesized following Schwertmann and Cornell [14]. The synthetic γ -AlOOH was prepared by alkaline precipitation of $\text{Al}(\text{NO}_3)_3$, aging for 48 h, repeatedly rinsing, and drying. All of these oxo-hydroxides were rinsed repeatedly with boiled distilled water until the pH of the suspension reached constant. The crystallite structures were examined with an X-ray diffractometer (D/MAX-rA, Rigaku). Catalyst particles with a diameter in the range of 0.075–0.3 mm were used in the experiments.

2.2. Surface characterization

The density of surface hydroxyl groups was measured according to a saturated deprotonation method that has been proved to be creditable [15,16]. It is a process of surface acid–base reaction for saturation. In detail, 0.3 g of oxide particles were added to a series of NaOH solutions (50 mL each, with concentrations ranging from 2 to 100 mM). After being shaken at 25 °C for more than 4 h, the solution was filtered with 0.45- μm acetate membrane. The supernatant was titrated with a standard HNO_3 solution to determine the residual NaOH. As the acidic hydroxyl groups react with NaOH, their density can be readily quantified by the NaOH consumption. Based on the principle of charge balance, the acidic and basic hydroxyl groups should be quantitatively equal. Thus, the total density of the surface hydroxyl groups is two times that of the acidic ones.

The pH_{pzc} (pH at which the surface is zero charged) was measured following a powder addition method [17,18,19]. To determine the intrinsic surface acidity constants, $\text{p}K_{\text{a}1}^{\text{int}}$ and $\text{p}K_{\text{a}2}^{\text{int}}$, the synthetic α -FeOOH was titrated with acid and base under nitrogen atmosphere following the method described by Stumm [17]. The specific surface area and pore volume of the catalyst particles were determined by adsorption and desorption of nitrogen on an automated gas sorption system (Autosorb-1, Quantachrome Corp.).

2.3. Chemical analysis

NB with low initial concentrations (tens of $\mu\text{g L}^{-1}$) was analyzed by GC/ECD (GC: 4890D, Agilent) equipped with a capillary column (HP-5, 30 m \times 0.53 mm \times 0.88 μm) [20]. The relative standard deviation (RSD) of the analysis was determined to be less than 5%. NB with high initial concentrations (hundreds of $\mu\text{g L}^{-1}$) was analyzed by a Waters HPLC system (717 plus Autosampler, 1525 Binary Pump, and 2478 Dual λ Absorbance Detector) with a Symmetry C18 column (3.9 mm \times 150 mm, Waters) at $\lambda = 260 \text{ nm}$. The eluent was a 70:30 (Milli-Q water/methanol) mixture. Aqueous ozone concentration was measured with the indigo method [21].

The concentrations of sulfate and phosphate after the adsorption by the α -FeOOH were determined using a Dionex ICS-1000 ion chromatography equipped with an IonPac AS-14 column and a conductivity detector. The eluent was a solution of 3.5 mM Na_2CO_3 /1.0 mM NaHCO_3 at a flow rate of 1.2 mL min^{-1} .

2.4. ATR-FTIR analysis

The oxo-hydroxides were dried previously at 110 °C for more than 12 h to remove adsorbed water molecules. To prepare an ATR sample, a desired amount of the pre-dried oxo-hydroxide particles were added into D_2O (99.8%, Acros) under nitrogen atmosphere to reach a slurry concentration of 67 g L^{-1} . The suspension was sealed and sonicated intermittently for 24 h, and aliquots were withdrawn for ATR-FTIR analysis.

Infrared spectra were obtained using a Nicolet 6500 FTIR spectrometer with a DTGS detector and a ZnSe ATR cell. Spectra over the 4000–650 cm^{-1} range were obtained by the co-addition of 128 scans under the analytical conditions of resolution 4 cm^{-1} , mirror velocity 0.6329 cm s^{-1} , gain 4, and aperture 150.

2.5. Experimental procedures

Ozonation experiments were carried out in batch mode at ambient temperatures. The glass reactor was cylindrical with a diameter of 6 cm and a volume of 1000 mL. Ozone gas was generated from dried oxygen using a laboratory ozone generator (XFZ-58I Tsinghua Tongli). After the generator reached a steady state, ozone gas was bubbled into distilled water in the reactor with a silica dispenser for a desired period of time. The initial aqueous ozone concentration can be controlled by changing the electrical current of the ozone generator. Then, the ozone gas was shut off. The stock solution of NB and the catalyst were quickly introduced into the reactor. The reactor was instantly sealed and the magnetic stirrer was turned on to initiate the catalytic ozonation experiments. Samples were withdrawn at pre-selected reaction times. After the residual ozone was instantly quenched with Na_2SO_3 solution (pre-acidified with sulfuric acid to pH 5), the samples were filtered through a 0.45- μm cellulose acetate membrane. Our preliminary experiments had shown that NB would not

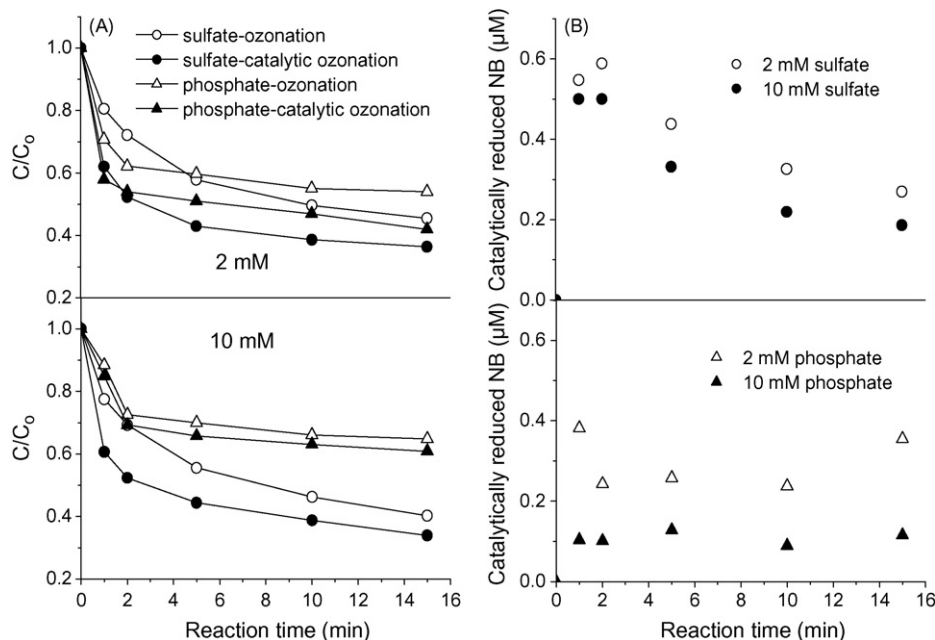


Fig. 1. Effect of sulfate and phosphate concentrations on the activity of α -FeOOH in oxidative degradation of NB: (A) NB degradation in the presence of 2 or 10 mM sulfate and phosphate; (B) catalytically reduced NB concentration vs. reaction time. Experimental conditions: pH_0 7.3, $[\text{O}_3]_0 = 1.20 \text{ mg L}^{-1}$, $[\text{NB}]_0 = 2.96 \mu\text{M}$, α -FeOOH dose = 200 mg L^{-1} , $T = 16^\circ\text{C}$.

evaporate under the magnetic stirring condition, and the sample filtration did not reduce the NB concentration.

3. Results and discussion

3.1. Active sites of α -FeOOH

Fig. 1 shows the effect of 2 and 10 mM sulfate and phosphate on the catalytic activity of α -FeOOH through the oxidative degradation of NB with ozonation alone and catalytic ozonation (O_3/α -FeOOH). Results indicate that catalytic ozonation could degrade NB more effectively than ozonation alone even in the presence of sulfate or phosphate (Fig. 1A). However, if the catalytically enhanced reduction of NB was considered (i.e., the difference of NB concentrations removed by catalytic ozonation and ozonation), phosphate inhibited the catalytic activity of α -FeOOH more significantly than sulfate (Fig. 1B). Furthermore, the inhibition on the catalyst increased with the increasing concentration of sulfate or phosphate. It seems that some interaction between the surface hydroxyl groups of α -FeOOH and sulfate or phosphate occurred, which suppressed the decomposition of aqueous ozone to produce $\cdot\text{OH}$.

Fig. 2 shows that the adsorbed amount of sulfate or phosphate on α -FeOOH increased with their increasing initial concentrations. In addition, more phosphate got adsorbed on α -FeOOH than sulfate at the same initial concentration. The interaction between the surface hydroxyl groups of α -FeOOH and the background anions can be examined by the FTIR spectrum of solid/water interface using an ATR accessory [22,23]. The stretching bands of the surface hydroxyl groups of hydroxylated α -FeOOH are usually covered up by the stronger ones of its bulk OH at around $3100\text{--}3200 \text{ cm}^{-1}$ and the surface hydrogen-bonded H_2O at $3200\text{--}3500 \text{ cm}^{-1}$. According to

Tejedor-Tejedor and Anderson [22], the stretching band of the bulk OH of α -FeOOH (at about 3145 cm^{-1}) could be separated from that of the surface OH by using D_2O as solvent to replace H_2O . These authors reported that the stretching band of the surface FeO-D was located at about 2642 cm^{-1} . Fig. 3 shows the effect of sulfate and phosphate on the ATR-FTIR spectra of α -FeOOH in D_2O suspension. The stretching band of the surface FeO-D was at about 2523 cm^{-1} (Fig. 3a), which is somewhat different from that reported by Tejedor-Tejedor and Anderson [22] probably due to different procedures for synthesizing α -FeOOH. After 67 mM sulfate or phosphate was added into D_2O suspension, the stretching band of FeO-D was significantly weakened by sulfate (Fig. 3b) or even

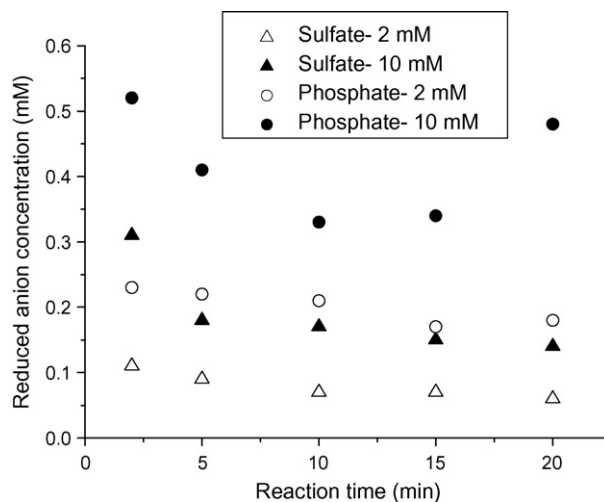


Fig. 2. Adsorption of sulfate or phosphate on α -FeOOH as a function of reaction time. Experimental conditions: pH_0 7.3, α -FeOOH dose = 200 mg L^{-1} , $T = 18^\circ\text{C}$.

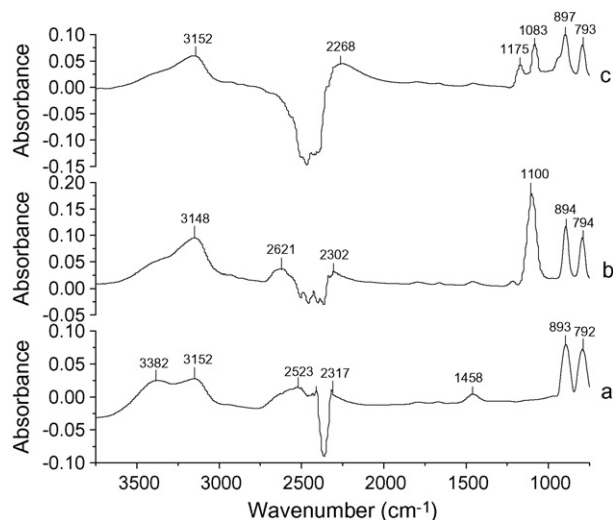


Fig. 3. Effect of sulfate and phosphate on ATR-FTIR spectra of α -FeOOH in D_2O suspension: (a) no anion added; (b) sulfate; (c) phosphate. The spectrum of D_2O has been subtracted from all the above spectra. D_2O vibrates at a stretching frequency of around 2435 cm^{-1} and a bending frequency of 1200 cm^{-1} . Experimental conditions: α -FeOOH dose = 67 g L^{-1} , $[SO_4^{2-}]$ or $[PO_4^{3-}] = 67\text{ mM}$.

completely eliminated by phosphate (Fig. 3c). It implies that both sulfate and phosphate could substitute the surface hydroxyl groups of α -FeOOH, while the effect of phosphate substitution was more notable. This result agrees well with the foregoing finding that phosphate inhibited the catalytic activity of α -FeOOH more significantly than sulfate. Therefore, it is reasonably proposed that the surface hydroxyl groups are the active sites of α -FeOOH in promoting $\bullet OH$ generation from aqueous ozone.

3.2. Comparison of the catalytic activities of several oxo-hydroxides

The surfaces of the synthetic α -FeOOH, β -FeOOH, γ -FeOOH, and γ -AlOOH are readily hydroxylated once suspended in water. The surface characteristics of the above oxo-hydroxides are summarized in Table 1, including the surface hydroxyl density in water, pH_{pzc} , BET surface area, and volume of pores. Results indicate that all the oxo-hydroxides could catalytically enhance NB degradation in comparison to ozonation alone, and their catalytic activities follow the increasing order of γ -AlOOH < γ -FeOOH < β -FeOOH < α -FeOOH (Fig. 4). However, their surface hydroxyl densities

Table 1
Major surface characteristics of selected catalysts

Catalyst	Surface hydroxyl density in water (mmol g^{-1})	pH_{pzc}	BET surface area ($\text{m}^2\text{ g}^{-1}$)	Pore volume (mL g^{-1}) ^a
α -FeOOH	0.50	7.0	68.4	0.25
β -FeOOH	1.21	7.3	132.4	0.27
γ -FeOOH	0.74	6.6	100.3	0.63
γ -AlOOH	1.15	7.5	120.1	0.14

^a For pores having a diameter in the range of 1.7–300 nm.

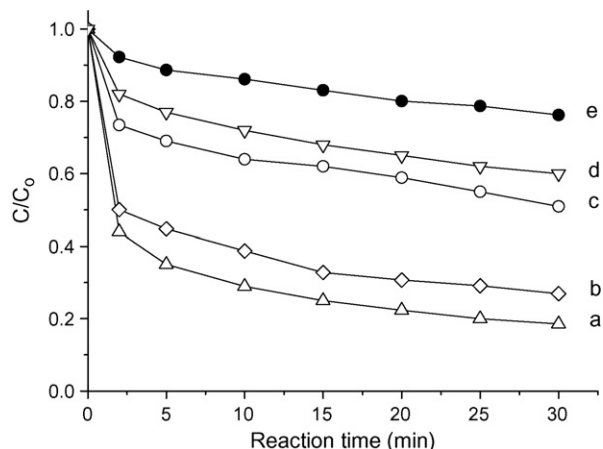


Fig. 4. Effect of catalyst type on oxidative degradation of NB: (a) O_3/α -FeOOH; (b) O_3/β -FeOOH; (c) O_3/γ -FeOOH; (d) O_3/γ -AlOOH; (e) O_3 alone. Experimental conditions: $[O_3]_0 = 0.82\text{ mg L}^{-1}$, $[NB]_0 = 2.88\text{ }\mu\text{M}$, catalyst dose = 100 mg L^{-1} , $pH_0 = 6.8$, $T = 18\text{ }^\circ\text{C}$.

follow the increasing order of α -FeOOH < γ -FeOOH < γ -AlOOH < β -FeOOH. Therefore, no correlation could be established between the surface hydroxyl densities and the catalytic activities of the oxo-hydroxides although the surface hydroxyl groups were found to be the active sites in promoting $\bullet OH$ generation. In addition, there was no correlation between other surface characteristics (i.e., surface area, pore volume) and the catalytic activities of the oxo-hydroxides.

Because NB reacts with both ozone molecule and $\bullet OH$ in ozonation and catalytic ozonation, its degradation can be expressed as:

$$-\frac{d[NB]}{dt} = k_1[O_3][NB] + k_2[\bullet OH][NB] \quad (1)$$

The reaction rate constants, k_1 and k_2 , are 0.09 and $4.0 \times 10^9\text{ M}^{-1}\text{ s}^{-1}$, respectively [12,24]. Aqueous ozone decomposition can be described as a pseudo-first order reaction in many cases especially when distilled water is used as background. The pseudo-first order reaction is also suitable to describe the ozone decomposition in ozonation and catalytic ozonation of this work:

$$-\frac{d[O_3]}{dt} = k[O_3] \quad (2)$$

where k is the rate constant of ozone decomposition. Transformation of the above equation leads to:

$$[O_3] = [O_3]_0 e^{-kt} \quad (3)$$

As recommended by von Gunten and Elovitz, a R_c value can be utilized to describe the molar concentration ratio of $\bullet OH$ to ozone during ozonation:

$$\frac{[\bullet OH]}{[O_3]} = R_c \quad (4)$$

The R_c value remains constant during ozonation of a water sample under a certain reaction condition (e.g., ozone dosage, pH, DOC, and temperature) [1,25]. The R_c concept is used for

both ozonation and catalytic ozonation here. Then, the concentration of hydroxyl radicals during the reactions can also be expressed as a function of reaction time. Consequently, NB concentration at a specific reaction time (t) can be described by Eq. (5):

$$\ln \frac{[\text{NB}]}{[\text{NB}]_0} = \frac{k_1 + k_2 R_c}{k} (e^{-kt} - 1) [\text{O}_3]_0 \quad (5)$$

Through fitting the experimental data shown in Fig. 4 with the above mathematical model, the R_c values in ozonation and catalytic ozonation are obtained and summarized in Table 2. The high r^2 values donate a good model-fitting. Results indicate that all the catalytic ozonation modes achieved a higher R_c value than ozonation alone. In addition, the R_c values of $\text{O}_3/\alpha\text{-FeOOH}$ and $\text{O}_3/\beta\text{-FeOOH}$ were notably higher than those of $\text{O}_3/\gamma\text{-FeOOH}$ and $\text{O}_3/\gamma\text{-AlOOH}$. Again, the result indicates that a high surface hydroxyl density did not necessarily lead to a high catalytic activity in promoting $\bullet\text{OH}$ generation from aqueous ozone. Not all surface hydroxyl groups of the oxo-hydroxides possessed the same high activity in the catalytic ozonation process. The catalytic activity of the oxo-hydroxides seems to correlate with some specific properties of their surface hydroxyl groups.

The properties of the surface hydroxyl groups of these hydroxylated oxo-hydroxides were further examined with the ATR-FTIR technique. The ATR-FTIR spectra of these oxo-hydroxides in D_2O suspensions are shown in Fig. 5 at similar pD values. Results show that the stretching bands of surface MeO-D of the $\alpha\text{-FeOOH}$, $\beta\text{-FeOOH}$, $\gamma\text{-FeOOH}$, and $\gamma\text{-AlOOH}$ were located at 2523, 2568, 2608, and 2642 cm^{-1} , respectively. The stretching bands at 2306–2319 cm^{-1} were ascribed to the hydrogen-bonded D_2O at the solid/ D_2O interface. The band at 2340–2360 cm^{-1} was due to the stretching vibration of atmospheric CO_2 . It is clear that the stretching frequencies of the surface MeO-D bonds followed the increasing order of $\alpha\text{-FeOOH} < \beta\text{-FeOOH} < \gamma\text{-FeOOH} < \gamma\text{-AlOOH}$, which accords with the reverse order of the catalytic activities of these oxo-hydroxides.

The relatively weak surface FeO-H bonds of $\alpha\text{-FeOOH}$ and $\beta\text{-FeOOH}$ seemed to favor the interaction of surface hydroxyl groups with aqueous ozone. As a dipole molecule, ozone has both nucleophilic site and electrophilic site [26]. Ozone molecule may combine with the H (electrophilic) and O (nucleophilic) atoms of the surface hydroxyl group during their interaction. The combination would enhance ozone decomposition thus promoting $\bullet\text{OH}$ generation. The relatively weak surface FeO-H bonds of

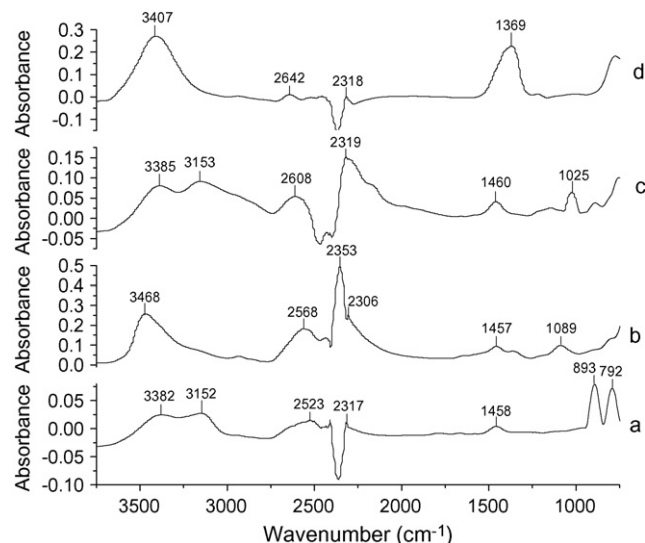
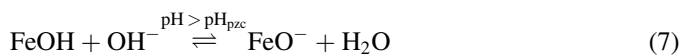


Fig. 5. ATR-FTIR spectra of catalysts in D_2O suspension: (a) $\alpha\text{-FeOOH}$; (b) $\beta\text{-FeOOH}$; (c) $\gamma\text{-FeOOH}$; (d) $\gamma\text{-AlOOH}$. The spectrum of D_2O has been subtracted from all the above spectra. D_2O vibrates at a stretching frequency of around 2435 cm^{-1} and a bending frequency of 1200 cm^{-1} . Experimental condition: $\text{pD}_0 = 6.8$, catalyst dose = 67 g L^{-1} .

the hydroxylated $\alpha\text{-FeOOH}$ lead to a high affinity of its electrophilic H and nucleophilic O for molecular ozone, which makes it easy for the surface OH –ozone combination. Therefore, the surface hydroxyl groups of the $\alpha\text{-FeOOH}$ exhibited higher catalytic activity than other oxo-hydroxides in promoting ozone decomposition to generate $\bullet\text{OH}$.

3.3. Role of charge status of surface hydroxyl groups

The charge state of surface hydroxyl groups depends on both water pH and pH_{pzc} of the catalyst. Most of the surface hydroxyl groups are at neutral state when water pH is close to the pH_{pzc} . Otherwise, protonated or deprotonated surface hydroxyl groups predominate when the water pH is far below or far above the pH_{pzc} (Eqs. (6) and (7)) [17].



The effect of water pH on NB degradation with O_3 and $\text{O}_3/\alpha\text{-FeOOH}$ is shown in Fig. 6A, and the corresponding R_c values ($r^2 > 0.96$) under different pH conditions are summarized in Fig. 6B. Similar to that reported in a former work [27], the water pH significantly affected the degradation of NB since OH^- can initiate ozone decomposition to generate $\bullet\text{OH}$ (Fig. 6A). In addition, $\alpha\text{-FeOOH}$ exhibited a high catalytic activity (achieved higher R_c than ozonation alone) over the pH range of 6.4–7.5, particularly at pH 6.9. As the water pH either decreased to 4.0 or increased to 9.0, the catalytic activity of $\alpha\text{-FeOOH}$ got decreased (Fig. 6B).

From the titration curve of $\alpha\text{-FeOOH}$ (Fig. 7A), the intrinsic acidity constants, $\text{p}K_{\text{a1}}^{\text{int}}$ and $\text{p}K_{\text{a2}}^{\text{int}}$, could be obtained by linear extrapolation following the method of Stumm [17] (Fig. 7B).

Table 2

Simulated R_c values of ozonation and catalytic ozonation

Ozonation mode	R_c	r^2
O_3	$(7.34 \pm 1.27) \times 10^{-9}$	0.96
$\text{O}_3/\alpha\text{-FeOOH}$	$(1.11 \pm 0.22) \times 10^{-7}$	0.95
$\text{O}_3/\beta\text{-FeOOH}$	$(9.27 \pm 2.11) \times 10^{-8}$	0.94
$\text{O}_3/\gamma\text{-FeOOH}$	$(4.13 \pm 1.01) \times 10^{-8}$	0.93
$\text{O}_3/\gamma\text{-AlOOH}$	$(2.02 \pm 0.39) \times 10^{-8}$	0.95

Experimental conditions: $[\text{O}_3]_0 = 0.82 \text{ mg L}^{-1}$, $[\text{NB}]_0 = 2.88 \text{ }\mu\text{M}$, catalyst dose = 100 mg L^{-1} , $\text{pH}_0 = 6.8$, $T = 18 \text{ }^\circ\text{C}$.

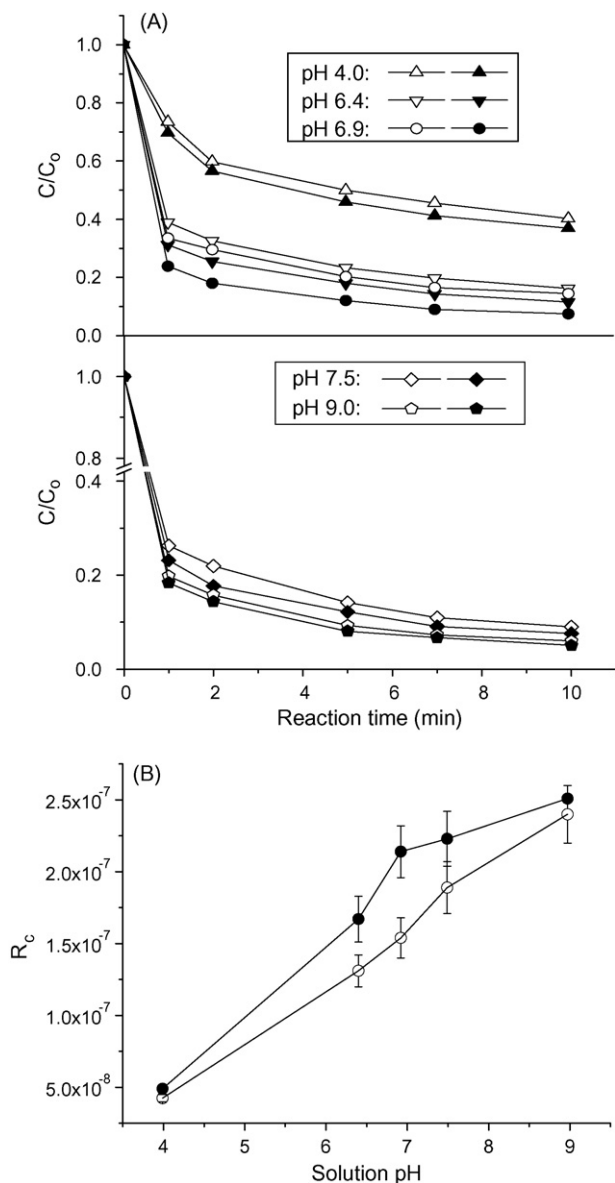


Fig. 6. Effect of pH on oxidative degradation of NB: (A) NB concentration vs. reaction time; (B) R_e values vs. solution pH. Open symbols: O_3 ; solid symbols: $O_3/\alpha\text{-FeOOH}$. Experimental conditions: $[O_3]_0 = 1.66 \text{ mg L}^{-1}$, $[NB]_0 = 1.58 \text{ }\mu\text{M}$, $\alpha\text{-FeOOH}$ dose = 100 mg L^{-1} , $T = 22 \text{ }^\circ\text{C}$.

The net surface charge was calculated from the difference between the total added base or acid and the equilibrium OH^- or H^+ concentration for a given amount of metal oxide used. The pK_{a1}^{int} and pK_{a2}^{int} of $\alpha\text{-FeOOH}$ were thus determined to be 5.5 and 8.6, respectively (Fig. 7B). With the intrinsic acidity constants available, the fractions of various surface hydroxyl species with different charge states could be readily plotted as a function of pH (Fig. 8). Results indicate that in the pH range of 6.4–7.5, more than 90% of the total surface hydroxyl groups were at the neutral state, which correlates with the high catalytic activity of $\alpha\text{-FeOOH}$ as described above. At pH values of 4.0 and 9.0, the protonated and deprotonated surface hydroxyl species would predominate, respectively, which correlates with the low catalytic activity of $\alpha\text{-FeOOH}$. Therefore, it is clear that the neutral surface hydroxyl species

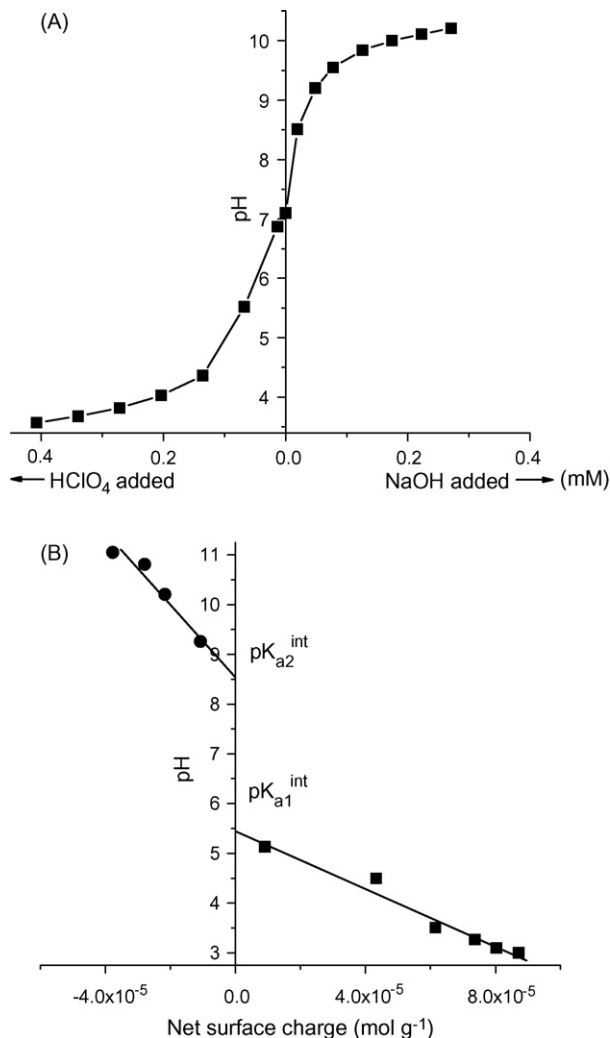


Fig. 7. Determination of intrinsic pK_a values of $\alpha\text{-FeOOH}$: (A) titration curve; (B) pH vs. net surface charge. Experimental condition: $\alpha\text{-FeOOH}$ dose = 1.5 g L^{-1} .

is most active in catalyzing ozone decomposition to generate $\bullet OH$. This phenomenon can be interpreted by the surface interaction mechanism proposed in Section 3.2. Since the protonation weakens the nucleophilicity of the O of surface

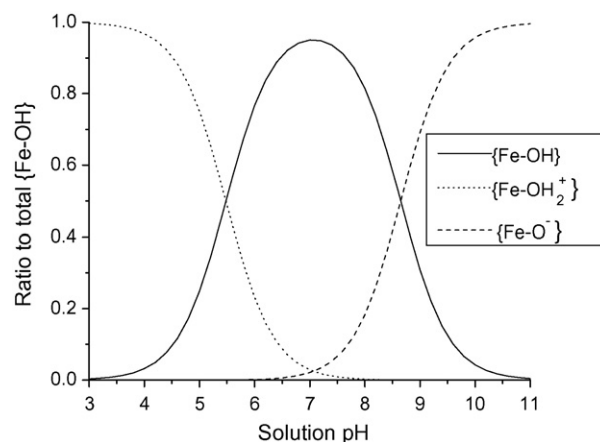


Fig. 8. Distribution of different surface hydroxyl species of $\alpha\text{-FeOOH}$ as a function of pH.

hydroxyl groups, the low solution pH consequently would decrease the interaction of the surface hydroxyl groups with ozone. At high pH, most of the electrophilic H of surface hydroxyl groups gets released into the solution thus reducing the chances of the surface OH–ozone interaction, which consequently leads to the low activity of the α -FeOOH in catalyzing \bullet OH generation.

The water pH is generally around neutral in most cases of water treatment, so α -FeOOH is a suitable catalyst to promote \bullet OH generation and enhance the degradation of refractory organic pollutants. This is the value of the catalytic ozonation with α -FeOOH in water treatment.

4. Conclusions

The work has revealed that surface hydroxyl groups of the hydroxylated α -FeOOH were important active sites in promoting \bullet OH generation from aqueous ozone. However, not all surface hydroxyl groups of the studied oxo-hydroxides possessed high activity in promoting \bullet OH generation. On the contrary, their catalytic activity was pertinent to the property of the surface MeO–H bonds. The surface hydroxyl groups of α -FeOOH exhibited a higher catalytic activity than those of other oxo-hydroxides (i.e., β -FeOOH, γ -FeOOH, and γ -AlOOH), which accorded well with its weaker surface MeO–H bond. A weaker surface MeO–H bond resulted in a stronger electrophilic H and nucleophilic O, which would facilitate the interaction between the surface hydroxyl group and the dipole molecule of ozone to promote \bullet OH generation. The surface OH–ozone interaction can well explain why the neutral surface hydroxyl species of α -FeOOH was highly active in catalyzing \bullet OH generation from aqueous ozone.

Acknowledgments

The financial support from the National Natural Science Foundation of China is greatly appreciated (No. 50578051 and

No. 50621804). We also thank Jinfeng Lu and Qun Wang at Harbin Institute of Technology for their help on experiments.

References

- [1] U. von Gunten, *Water Res.* 37 (2003) 1443.
- [2] Z. Qiang, C. Adams, R. Surampalli, *Ozone-Sci. Eng.* 26 (2004) 525.
- [3] J. Ma, N.J.D. Graham, *Water Res.* 33 (1999) 785.
- [4] M. Ernst, F. Lurot, J.C. Schrotter, *Appl. Catal. B: Environ.* 47 (2004) 15.
- [5] J.S. Park, H. Choi, J. Cho, *Water Res.* 38 (2004) 2285.
- [6] R. Andreozzi, A. Insola, V. Caprio, R. Marotta, V. Tufano, *Appl. Catal. A: Gen.* 138 (1996) 75.
- [7] F.J. Beltrán, F.J. Rivas, R. Montero-de-Espinosa, *Ind. Eng. Chem. Res.* 24 (2003) 3218.
- [8] B. Kasprzyk-Hordern, M. Ziólek, J. Nawrocki, *Appl. Catal. B: Environ.* 46 (2003) 639.
- [9] Y. Joseph, W. Ranke, W. Weiss, *J. Phys. Chem. B.* 104 (2000) 3224.
- [10] D.A. Dzombak, F.M.M. Morel, *Surface Complexation Modeling*, John Wiley & Sons, New York, 1990, p. 45–47.
- [11] H.N. Lim, H. Choi, T.M. Hwang, J.W. Kang, *Water Res.* 36 (2002) 219.
- [12] J. Hoigné, H. Bader, *Water Res.* 17 (1983) 173.
- [13] K. Kandori, M. Fukuoka, T. Ishikawa, *J. Mater. Sci.* 26 (1991) 3313.
- [14] U. Schwertmann, R. Cornell, *Iron Oxides in the Laboratory: Preparation and Characterization*, Wiley-VCH, Weinheim, 2000, p. 93–118.
- [15] E. Laiti, L.O. Öhman, J. Nordin, S. Sjöberg, *J. Colloid Interface Sci.* 175 (1995) 230.
- [16] H. Tamura, A. Tanaka, K. Mita, R. Furuichi, *J. Colloid Interface Sci.* 209 (1999) 225.
- [17] W. Stumm, *Chemistry of the Soil-Water Interface*, John Wiley & Sons, New York, 1992, p. 15–20.
- [18] G. Newcombe, R. Hayes, M. Drikas, *Colloid Surf. A* 78 (1993) 65.
- [19] M. Mullet, P. Fievet, A. Szymczyk, A. Foissy, J.C. Reggiani, J. Pagetti, *Desalination* 121 (1999) 41.
- [20] J. Ma, M. Sui, T. Zhang, C. Guan, X. Bao, *Water Res.* 39 (2005) 779.
- [21] H. Bader, J. Hoigné, *Water Res.* 15 (1981) 449.
- [22] M.I. Tejedor-Tejedor, M.A. Anderson, *Langmuir* 2 (1986) 203.
- [23] M.I. Tejedor-Tejedor, M.A. Anderson, *Langmuir* 6 (1990) 602.
- [24] V.B. George, *J. Phys. Chem. Ref. Data* 17 (1988) 513.
- [25] M.S. Elovitz, U. von Gunten, *Ozone Sci. Eng.* 21 (1999) 239.
- [26] F.J. Beltrán, *Ozone Reaction Kinetics for Water and Wastewater Systems*, Lewis Publisher, Boca Raton, 2004, p. 3–4.
- [27] J. Ma, T. Zhang, Z. Chen, M. Sui, X. Li, *Environ. Sci.* 26 (2005) 78 (in Chinese).